Editors' Suggestion

Energy-Dependent $\pi^+\pi^+\pi^+$ Scattering Amplitude from QCD

Maxwell T. Hansen,[1,2,*] Raul A. Briceño,[3,4,†] Robert G. Edwards,[3,‡]
Christopher E. Thomas,[5,§] and David J. Wilson[5,‖]

(for the Hadron Spectrum Collaboration)

[1]*Theoretical Physics Department, CERN, 1211 Geneva 23, Switzerland*
[2]*Higgs Centre for Theoretical Physics, School of Physics and Astronomy, The University of Edinburgh, Edinburgh EH9 3FD, United Kingdom*
[3]*Thomas Jefferson National Accelerator Facility, 12000 Jefferson Avenue, Newport News, Virginia 23606, USA*
[4]*Department of Physics, Old Dominion University, Norfolk, Virginia 23529, USA*
[5]*DAMTP, University of Cambridge, Wilberforce Road, Cambridge CB3 0WA, United Kingdom*

(Received 8 October 2020; accepted 6 November 2020; published 5 January 2021)

Focusing on three-pion states with maximal isospin ($\pi^+\pi^+\pi^+$), we present the first nonperturbative determination of an energy-dependent three-hadron scattering amplitude from first-principles QCD. The calculation combines finite-volume three-hadron energies, extracted using numerical lattice QCD, with a relativistic finite-volume formalism, required to interpret the results. To fully implement the latter, we also solve integral equations that relate an intermediate three-body K matrix to the physical three-hadron scattering amplitude. The resulting amplitude shows rich analytic structure and a complicated dependence on the two-pion invariant masses, represented here via Dalitz-like plots of the scattering rate.

DOI: 10.1103/PhysRevLett.126.012001

Introduction.—The three-body problem lies at the core of a broad range of outstanding questions in quantum chromodynamics (QCD). The largest uncertainty in QCD-based structure calculations of light nuclei, for example, is the estimate of the three-nucleon force (see Ref. [1]). In addition, many QCD resonances have significant branching fraction to channels with three or more hadrons. The Roper resonance, for example, has defied simple quark-model descriptions, due in part to its nature as a broad resonance with a ~30% branching fraction to $N\pi\pi$. A rigorous QCD calculation would elucidate the role of nonperturbative dynamics in the Roper's peculiar properties, e.g., the fact that it has a lower mass than the negative-parity ground state, which seems unnatural from the perspective of the quark model [2,3].

As a necessary step towards studying a broad class of three-hadron systems, in this work we present the first study of an energy-dependent three-body scattering amplitude from QCD. This nonperturbative result is achieved by the coalescence of three novel techniques: a calculation of finite-volume three-hadron energies based in numerical lattice QCD, a relativistic finite-volume formalism to relate the energies to K matrices, and a numerical evaluation of corresponding integral equations to convert the latter into the three-hadron scattering amplitude. The theoretical basis required to achieve these final two steps was derived in Refs. [4,5]. (A large body of work has investigated general methods for relating finite-volume energies to scattering amplitudes for both two- and three-body states. See Refs. [6–24] and Refs. [25–45], respectively.)

This work considers the scattering of three-pion states with maximal isospin ($I = 3$) in QCD with three dynamical quarks ($N_f = 2 + 1$): two degenerate light quarks, with heavier-than-physical mass corresponding to a pion mass $m_\pi \approx 391$ MeV, and a strange quark. This channel offers an optimal benchmark case, since both the maximal-isospin three-pion system and its two-pion subsystem are expected to be weakly interacting and nonresonant.

Many numerical studies of three-hadron states have been published over the last decade, ranging from early work deriving and fitting large-volume expansions of the three-pion ground state [46–48] to more recent results using quantization conditions to study ground [49] and excited states [50–52], with the latter set each analyzing the lattice QCD spectrum published in Ref. [53]. Independent sets of finite-volume energies have also been calculated and analyzed in Refs. [54] and [55]. The present investigation goes beyond this previous work, by providing the first complete numerical determination of physical scattering amplitudes for three-body systems.

In the following, we first discuss our determination of two- and three-pion finite-volume energies, before describing the fits used to relate these to infinite-volume K matrices. The latter then serve as inputs to known integral equations, which we solve numerically to extract the $3\pi^+ \to 3\pi^+$ scattering amplitude. Additional details of the analysis are discussed in the Supplemental Material [56].

Spectral determination.—Figure 1 summarizes the two- and three-pion finite-volume spectra calculated in this work. Two-pion energies on the larger volume have already appeared in Ref. [57].

Computations were performed on anisotropic lattices which have a temporal lattice spacing, a_t, finer than the spatial lattice spacing, a_s [$a_t = a_s/\xi$ with $\xi = 3.444(6)$ [57]]. Two lattice ensembles were used, differing only in the volume: $(L/a_s)^3 \times (T/a_t) = 20^3 \times 256$ (with 256 gauge-field configurations) and $24^3 \times 128$ (with 512 configurations). We use $2+1$ flavors of dynamical clover fermions, with three-dimensional stout-link smearing in the fermion action, and a tree-level Symanzik-improved gauge action. The bare parameters and basic lattice properties are detailed in Refs. [58,59]. Setting the scale via $a_t^{-1} = m_\Omega^{\rm exp}(a_t m_\Omega^{\rm latt})^{-1}$, [where $a_t m_\Omega^{\rm latt} = 0.2951(22)$ was measured in Ref. [60] and $m_\Omega^{\rm exp}$ is the experimentally determined Ω baryon mass from Ref. [61]] and combining with $a_t m_\pi = 0.06906(13)$ [57] and $a_t m_K = 0.09698(9)$ [62], yields $m_\pi \approx 391$ MeV and $m_K \approx 550$ MeV. The values of $a_t m_\pi$ and ξ translate into spatial extents of $m_\pi L = 4.76$ and $m_\pi L = 5.71$ for the two ensembles.

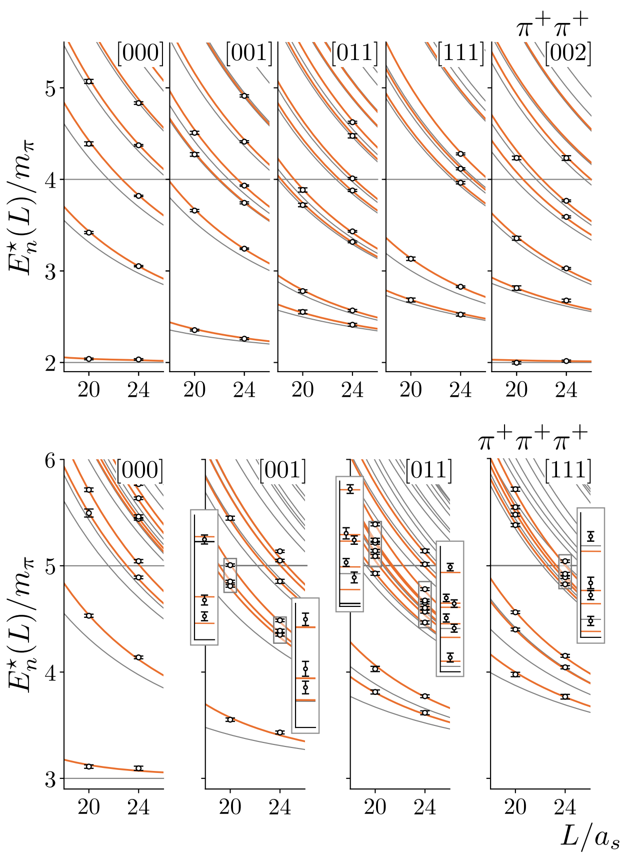

FIG. 1. The $\pi^+\pi^+$ and $\pi^+\pi^+\pi^+$ finite-volume spectra in the center-of-momentum frame for the relevant finite-volume irreps with various overall momenta, as explained in the text. Points are computed energy levels on the two volumes with error bars showing statistical uncertainties. Each rectangular inset shows a vertical zoom of the region indicated by the small neighboring rectangle. Gray curves are the "noninteracting" finite-volume energies, i.e., the energies in the absence of any interactions between pions. Orange curves are predictions from the finite-volume formalism based only on the two-particle scattering length, given in Eq. (4) (here with the local three-body interaction set to zero).

The spectrum of energies in a finite volume is discrete and each energy level provides a constraint on the scattering amplitudes at the corresponding center-of-momentum energy. To obtain more constraints, we compute spectra for systems with overall zero and nonzero momentum, $\boldsymbol{P}$. Momenta are quantized by the cubic spatial boundary conditions, $\boldsymbol{P} = (2\pi/L)(n_1, n_2, n_3)$, where $\{n_i\}$ are integers, and we write this using a shorthand notation as $[n_1 n_2 n_3]$.

In this work we restrict attention to S-wave scattering. The reduced symmetry of a cubic lattice means that total angular momentum J is not a good quantum number and instead channels are labeled by the irreducible representation (irrep, Λ) of the octahedral group with parity for $\boldsymbol{P} = \boldsymbol{0}$ or the relevant subgroup that leaves $\boldsymbol{P}$ invariant for $\boldsymbol{P} \neq \boldsymbol{0}$ [63,64]. We consider the relevant irreps which contain $J = 0$: $A_1^-(A_1^+)$ for $\pi\pi\pi\ (\pi\pi)$ at rest and $A_2(A_1)$ for $\pi\pi\pi\ (\pi\pi)$ with nonzero $\boldsymbol{P}$. Isospin I and G parity G are good quantum numbers in our lattice formulation; these distinguish the two-pion ($I^G = 2^+$) and three-pion ($I^G = 3^-$) channels. We neglect higher partial waves here, in particular the two-particle D wave that mixes with the S wave in the finite-volume energies. As described in Ref. [57], a nonzero D-wave interaction can be extracted, in particular, if aided by the consideration of other, nontrivial finite-volume irreps, but has a small influence on the two-pion energies considered here. There is, in principle, a systematic uncertainty associated with neglecting the D-wave contribution. Given the consistency of our results with Ref. [57], this appears to be below the statistical uncertainty in the present fits. See also Secs. VIII A and B of that work for more discussion.

To reliably extract the finite-volume energies we have computed two-point correlation functions using a large basis of appropriate interpolating operators. From these, the spectra are determined using the variational method [65–67], with our implementation described in Refs. [68,69]. This amounts to calculating a matrix of correlation functions,

$$G_{ij}(t) = \langle \mathcal{O}_i(t) \mathcal{O}_j^\dagger(0) \rangle, \tag{1}$$

and diagonalizing $M(t, t_0) = G(t_0)^{-1/2} G(t) G(t_0)^{-1/2}$ for a fixed t_0. One can show that the corresponding eigenvalues satisfy $\lambda_n(t,t_0) \to e^{-E_n(L)(t-t_0)}$, where $E_n(L)$ is the nth energy level with overlap to some of the operators in the basis. This basic methodology has been applied to a wide range of two-hadron scattering observables for several phenomenologically interesting channels [57,70–81]. See Sec. I of the Supplemental Material [56] for some example plots of $\lambda_n(t,t_0)$.

In order to robustly interpolate the two- and three-pion energy eigenstates we use operators with two- and three-meson-like structures in the appropriate irrep, constructed from products of single-meson-like operators projected to definite spatial momentum. The latter are built from linear combinations, chosen to optimize overlap to the single-pion states, of fermion bilinears of the form, $\bar{\psi}\Gamma D \ldots D\psi$, where ψ is a quark field and D is a discretized covariant derivative. Details of these operator constructions are given in Sec. V of the Supplemental Material [56] with further details relevant to the three-meson-like operators presented in Ref. [82]. Using such a wide variety of optimized operators, and especially multihadron operators with momentum-projected single-hadron components, allows one to minimize excited state contamination and extract the energies reliably and precisely from small values of t. This approach is made feasible due to the distillation method [83] which we employ to efficiently compute the numerous quark-field Wick contractions that are required. We use 128 distillation vectors for the 20^3 ensemble and 162 for the 24^3.

Returning to the two- and three-pion spectra summarized in Fig. 1, we observe a one-to-one correspondence between the computed energy levels and the noninteracting energies in all panels, with the computed values slightly higher in energy than the noninteracting levels. This suggests that the system is weakly interacting and repulsive in both the two- and three-hadron sectors.

Analyzing the finite-volume spectra.—We now describe our method for determining two- and three-body K matrices from the extracted finite-volume energies, beginning with an overview of scattering observables:

The two-pion scattering amplitude is defined as the connected part of the overlap between an incoming $\pi^+\pi^+$ asymptotic state (with momenta $\boldsymbol{p}, -\boldsymbol{p}$) to an outgoing $\pi^+\pi^+$ state (with $\boldsymbol{p}', -\boldsymbol{p}'$). Without loss of generality, here we have assumed the center-of-momentum frame. We also define $p = |\boldsymbol{p}| = |\boldsymbol{p}'|$, where we have used that the magnitudes must be equal to satisfy energy conservation. In addition, $s_2 \equiv E_2^{\star 2} \equiv 4(p^2 + m_\pi^2)$ defines the squared center-of-momentum frame energy. The only remaining degree of freedom is the scattering angle between $\boldsymbol{p}$ and $\boldsymbol{p}'$. In this work we focus on the S-wave scattering amplitude, denoted $\mathcal{M}_2$, in which this angle is integrated to project onto zero-angular-momentum states. Finally we recall the simple relation between $\mathcal{M}_2$ and the K matrix in the elastic region, $\mathcal{K}_2^{-1} = \mathrm{Re}\mathcal{M}_2^{-1}$. The imaginary part of $\mathcal{M}_2^{-1}$ is completely fixed by unitarity so that $\mathcal{K}_2$ is the only part free to depend on the dynamics of the system. We work with the simple phase space factor, proportional to the momentum magnitude. See, e.g., Ref. [23] for more details. In contrast to $\mathcal{M}_2$, $\mathcal{K}_2$ is real for real s_2 and is meremorphic in a region of the complex s_2 plane around $s_2 = 4m_\pi^2$. In this work we also consider an analogous, three-body K matrix, introduced in Ref. [4] and denoted by $\mathcal{K}_{\mathrm{df},3}$.

In the two-pion sector, in the case that the S-wave interactions are dominant, the scalar-irrep finite-volume energies satisfy the quantization condition [6,7,9],

$$\mathcal{K}_2(E_2^\star) + F^{-1}(E_2, \boldsymbol{P}, L) = 0, \tag{2}$$

where $E_2^\star \equiv \sqrt{E_2^2 - \boldsymbol{P}^2}$ is the center-of-momentum energy and $F(E_2, \boldsymbol{P}, L)$ is a known geometric function. For the three-body sector, we use the isotropic approximation of the general formalism derived in Ref. [4], which takes an analogous form, now for pseudoscalar-irrep energies

$$\mathcal{K}_{3,\mathsf{iso}}(E_3^\star) + F_{3,\mathsf{iso}}^{-1}[\mathcal{K}_2](E_3, \boldsymbol{P}, L) = 0, \tag{3}$$

where the notation is meant to stress that $F_{3,\mathsf{iso}}[\mathcal{K}_2](E_3, \boldsymbol{P}, L)$ is a functional of $\mathcal{K}_2(E_2^\star)$. $F_{3,\mathsf{iso}}$ is defined in Eq. (39) of Ref. [4]. Here $\mathcal{K}_{3,\mathsf{iso}}$ is the component of $\mathcal{K}_{\mathrm{df},3}$ that only depends on the total three-hadron energy, i.e., is "isotropic." Equation (3) holds only when $\mathcal{K}_{\mathrm{df},3}$ is well approximated to be isotropic and our fits give evidence that this is a good approximation for this system.

Combining these two conditions with the energies plotted in Fig. 1 allows one to constrain both the two- and three-hadron K matrices. One strategy is to fit a parametrization of $\mathcal{K}_2$ and use this to determine the energy dependence of $\mathcal{K}_{3,\mathsf{iso}}$ as summarized in Fig. 2. An alternative approach is to parametrize both K matrices and fit these simultaneously to the entire set of finite-volume energies. A detailed discussion with a wide range of fits is given in Sec. II of the Supplemental Material [56]. Both strategies give consistent results and the key message is that the full dataset is well described by a constant $\mathcal{K}_{3,\mathsf{iso}}$ that is consistent with zero, together with the leading-order effective range expansion: $\tan\delta(p) = -a_0 p$ with $\mathcal{K}_2(E_2^\star) = -16\pi E_2^\star \tan\delta(p)/p$. Here the second equation defines the S-wave scattering phase shift $\delta(p)$, and the first defines the scattering length a_0. Our best fit, performed simultaneously to all spectra shown in Fig. 1 but with a cutoff in the center-of-momentum frame energies included, yields

$$\begin{aligned} m_\pi a_0 &= 0.296 \pm 0.008 \\ m_\pi^2 \mathcal{K}_{3,\mathsf{iso}} &= -339 \pm 770 \end{aligned} \quad \begin{bmatrix} 1.0 & 0.6 \\ & 1.0 \end{bmatrix}, \tag{4}$$

with a χ^2 per degree of freedom of $64.5/(37-2) = 1.84$. This fit is denoted by B_{2+3} in Sec. II of the Supplemental Material [56]. As explained there, the fitted data include all two-pion energies below $E_{2,\mathsf{cut}}^\star = 3.4 m_\pi$ and all three-pion energies below $E_{3,\mathsf{cut}}^\star = 4.4 m_\pi$, with both cutoffs

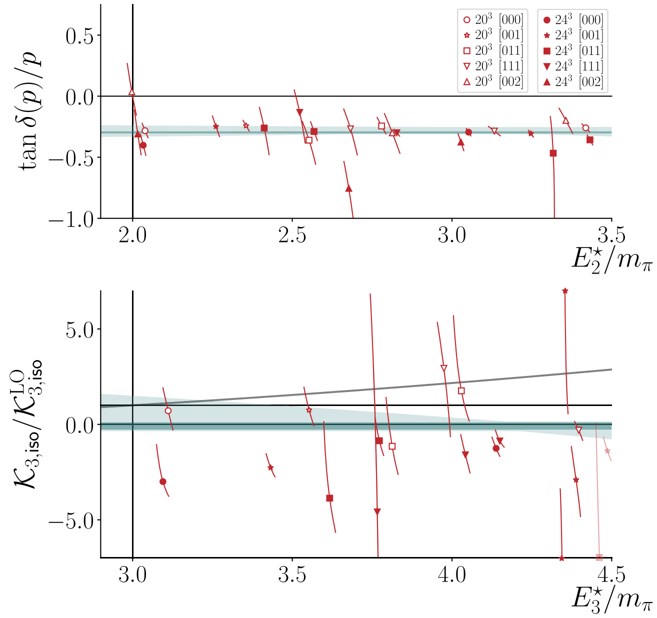

FIG. 2. Example of data and fits for $\mathcal{K}_2$ and $\mathcal{K}_{3,\mathrm{iso}}$, as described in the text. The red points are given by substituting finite-volume energies into $-1/F(E_2,\boldsymbol{P},L)$ and $-1/F_{3,\mathrm{iso}}(E_3,\boldsymbol{P},L)$ for the two- and three-particle energies, respectively, with the volume and $\boldsymbol{P}$ indicated in the legend. A symbol appearing at the very top or bottom represents a case where the central value falls outside the plotted region. The dark cyan bands represent the fit shown in Eq. (4) while the lighter bands show the spread covered by the various fits described in the Supplemental Material [56]. For the bottom panel we normalize to $m_\pi^2\mathcal{K}_{3,\mathrm{iso}}^{\mathrm{LO}} = 4608\pi^2(m_\pi a_0)^2$, with $m_\pi a_0$ taken from Eq. (4). This simple relation between $\mathcal{K}_{3,\mathrm{iso}}$ and the two-particle scattering length holds at leading order in chiral perturbation theory at threshold, as was first derived in Ref. [50]. The gray curve gives the full leading-order prediction, which is linear in $E_3^{\star 2}$.

applied to energies in the center-of-momentum frame. The square-bracketed matrix gives the correlation between the two fit parameters. This fit is consistent with the previous determination of the scattering length at this pion mass, presented in Ref. [57], and is also the value used to generate the orange curves in Fig. 1 (together with $\mathcal{K}_{3,\mathrm{iso}} = 0$). In Fig. 2 we illustrate the same fit using the darker cyan curves. In addition, we include the lighter bands as a systematic uncertainty, estimated from the spread of various constant and linear fits, as detailed in Sec. II of the Supplemental Material [56].

$3\pi^+$ *scattering amplitude.*—Following the relativistic integral equations presented in Ref. [5], we can write the $J=0$ and $\mathcal{K}_{3,\mathrm{iso}}=0$ amplitude as follows:

$$\mathcal{M}_3^{(u,u)}(p,k) = -\mathcal{M}_2(E_{2,p}^\star)G_{\mathsf{s}}(p,k)\mathcal{M}_2(E_{2,k}^\star) - \mathcal{M}_2(E_{2,p}^\star)\int_{k'} G_{\mathsf{s}}(p,k')\mathcal{M}_3^{(u,u)}(k',k), \quad (5)$$

where $\int_k \equiv \int dk k^2/[(2\pi)^2\omega_k]$ and we have introduced

$$G_{\mathsf{s}}(p,k) \equiv -\frac{H(p,k)}{4pk}\log\left[\frac{\alpha(p,k)-2pk+i\epsilon}{\alpha(p,k)+2pk+i\epsilon}\right], \quad (6)$$

$$\alpha(p,k) \equiv (E_3-\omega_k-\omega_p)^2 - p^2 - k^2 - m^2. \quad (7)$$

$\mathcal{M}_2$ is the S-wave two-particle scattering amplitude, introduced above, which depends on the invariant $E_{2,k}^{\star 2} \equiv (E_3-\omega_k)^2 - k^2$, with $\omega_k = \sqrt{k^2+m^2}$. The (u,u) superscript emphasizes that specific spectator momenta, k and p, are singled out in the initial and final states, respectively. The function G_{s} encodes the spectator exchange, projected to the S wave. It inherits a scheme dependence through the smooth cutoff function H, defined in Eqs. (28) and (29) of Ref. [4]. This scheme dependence is matched by that inside of $\mathcal{K}_{3,\mathrm{iso}}$ such that the resulting scattering amplitude is universal.

To use Eq. (5) in practice, one requires a parameterization for $\mathcal{M}_2$. As described in the previous section, the $\pi^+\pi^+$ system is well described using the leading order effective range expansion for $\mathcal{M}_2$,

$$\mathcal{M}_2(E_2^\star) = \frac{16\pi E_2^\star}{-1/a_0 - i\sqrt{E_2^{\star 2}/4 - m_\pi^2}}. \quad (8)$$

Following the derivation of Ref. [5], the final step is to symmetrize with respect to the spectators, to reach

$$\mathcal{M}_3(s_3, m_{12}'^2, m_{13}'^2, m_{12}^2, m_{13}^2) = \sum_{\boldsymbol{p}_i\in\mathcal{P}_p}\sum_{\boldsymbol{k}\in\mathcal{P}_k}\mathcal{M}_3^{(u,u)}(p,k), \quad (9)$$

where $\mathcal{P}_p = \{\boldsymbol{p}, \boldsymbol{a}', -\boldsymbol{p}-\boldsymbol{a}'\}$ and $\mathcal{P}_k = \{\boldsymbol{k}, \boldsymbol{a}, -\boldsymbol{k}-\boldsymbol{a}\}$. We have presented the left-hand side as a function of the five Lorentz invariants that survive after truncating to $J=0$ in both the two and three particle sector: the squared three-hadron center-of-momentum frame energy, s_3, as well as two pion-pair invariant masses for each of the initial and final states. These are defined by introducing the notation $\{\boldsymbol{k}, \boldsymbol{a}, -\boldsymbol{k}-\boldsymbol{a}\} = \{\boldsymbol{p}_1, \boldsymbol{p}_2, \boldsymbol{p}_3\}$, then, for example,

$$m_{12}^2 = (p_1+p_2)^2 = (E_3^\star - [m_\pi^2 + \boldsymbol{p}_3^2]^{1/2}) - \boldsymbol{p}_3^2, \quad (10)$$

where the middle expression depends on on-shell four-vectors with $p_1^2 = m_\pi^2$.

In the top panel of Fig. 3 we show a Dalitz-like plot of $|\mathcal{M}_3|^2$ as a function of (m_{12}, m_{13}), with all other kinematics fixed as indicated in the caption. In a usual Dalitz description, the incoming energy is fixed by the decaying particle so that only the outgoing kinematics can vary, whereas here we simply fix the other kinematics. The inputs to this plot are the best-fit scattering length, given in Eq. (4), together with $\mathcal{K}_{3,\mathrm{iso}} = 0$. The bottom panel of Fig. 3 shows the same $\sqrt{s_3}$ but varies incoming and outgoing kinematics according to $m_{12} = m_{12}'$ and $m_{13} = m_{13}'$.

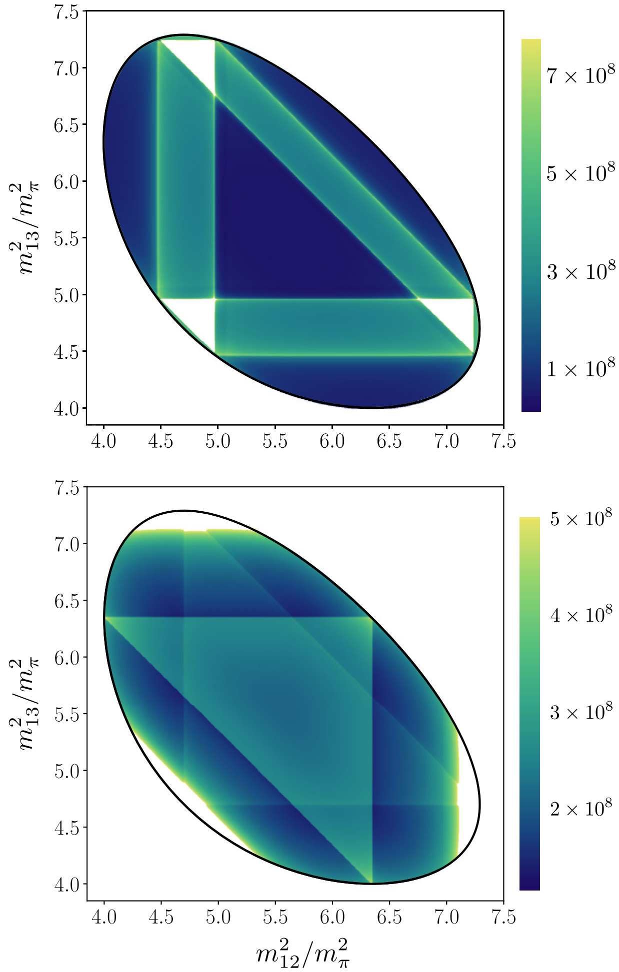

FIG. 3. Top: Dalitz-like plot of $m_\pi^4|\mathcal{M}_3|^2$ for $\sqrt{s_3} = 3.7m$ with final kinematics fixed to $\{\boldsymbol{p}_1'^2, \boldsymbol{p}_2'^2\} = \{0.01m_\pi^2, 0.7m_\pi^2\}$ $\Rightarrow \{m_{12}', m_{13}'\} = \{2.1m_\pi, 2.25m_\pi\}$. Bottom: Same total energy, now with incoming and outgoing kinematics set equal, as discussed in the text.

Additional details concerning the S-wave integral equations are presented in Secs. III and IV of the Supplemental Material [56], where we also describe the propagation of the uncertainties of $m_\pi a_0$ and $\mathcal{K}_{3,\mathrm{iso}}$ into the predicted amplitude. (See also Ref. [84] for more details on expressing the three-particle amplitude via a truncated partial wave series and Ref. [85] for a discussion of integral equations and their solutions in a resonant three-hadron channel.)

Summary.—In this work we have presented the first lattice QCD determination of the energy-dependent three-to-three scattering amplitude for three pions with maximal isospin. The calculation proceeded in three steps: (i) determining finite-volume energies with $\pi^+\pi^+\pi^+$ quantum numbers, (ii) using the framework of Ref. [4] to extract two- and three-body K matrices from these, and (iii) applying the results of Ref. [5] to convert these to the three-hadron scattering amplitude, by solving known integral equations. The three steps are summarized, respectively, by Figs. 1, 2, and 3.

Having established this general workflow, it is now well within reach to rigorously extract three-hadron resonance properties from lattice QCD calculations. In particular the formalism has recently been extended to three-pion states with any value of isospin in Ref. [42]. This should enable studies, for example, of the ω, h_1, and a_1 resonances. The main outstanding challenges here include rigorous resonant parametrizations of the intermediate three-body K matrix, as well as a better understanding of the analytic continuation required to identify the resonance pole position.

The authors would like to thank M. Bruno, J. Dudek, A. Jackura, L. Leskovec, and A. Rodas for useful conversations, as well as our other colleagues within the Hadron Spectrum Collaboration. R. A. B., R. G. E., and C. E. T. acknowledge support from the U.S. Department of Energy Contract No. DE-AC05-06OR23177, under which Jefferson Science Associates, LLC, manages and operates Jefferson Lab. R. A. B. also acknowledges support from the U.S. DOE Early Career Award, Contract No. de-sc0019229. C. E. T. and D. J. W. acknowledge support from the U.K. Science and Technology Facilities Council (STFC) (Grant No. ST/P000681/1). D. J. W. acknowledges support from a Royal Society University Research Fellowship. M. T. H., C. E. T. and D. J. W. acknowledge the MITP topical workshop “Scattering Amplitudes and Resonance Properties for Lattice QCD” for stimulating this project and for hospitality during the initial discussions. M. T. H. and C. E. T. also acknowledge the CERN-TH Institute “Advances in Lattice Gauge Theory,” which provided the opportunity to make significant progress on this work. C. E. T. further acknowledges CERN TH for hospitality and support during a visit in January and February of this year. The software codes CHROMA [86] and QUDA [87–89] were used. The authors acknowledge support from the U.S. Department of Energy, Office of Science, Office of Advanced Scientific Computing Research and Office of Nuclear Physics, Scientific Discovery through Advanced Computing (SciDAC) program. Also acknowledged is support from the U.S. Department of Energy Exascale Computing Project. This work was also performed on clusters at Jefferson Lab under the USQCD Collaboration and the LQCD ARRA Project. This research was supported in part under an ALCC award, and used resources of the Oak Ridge Leadership Computing Facility at the Oak Ridge National Laboratory, which is supported by the Office of Science of the U.S. Department of Energy under Contract No. DE-AC05-00OR22725. This research used resources of the National Energy Research Scientific Computing Center (NERSC), a DOE Office of Science User Facility supported by the Office of Science of the U.S. Department of Energy under Contract No. DE-AC02-05CH11231. The authors acknowledge the Texas Advanced Computing Center (TACC) at The University of Texas at Austin for providing HPC resources. Gauge configurations were generated using resources awarded from the U.S. Department of Energy INCITE program at the Oak Ridge Leadership Computing Facility, the NERSC, the NSF Teragrid at the TACC and the Pittsburgh Supercomputer Center, as well as at Jefferson Lab.

---

*maxwell.hansen@cern.ch
†rbriceno@jlab.org
‡edwards@jlab.org
§c.e.thomas@damtp.cam.ac.uk
‖d.j.wilson@damtp.cam.ac.uk

[1] M. Piarulli *et al.*, Phys. Rev. Lett. **120**, 052503 (2018).
[2] N. Isgur and G. Karl, Phys. Lett. **72B**, 109 (1977).
[3] N. Isgur and G. Karl, Phys. Rev. D **19**, 2653 (1979); **23**, 817(E) (1981).
[4] M. T. Hansen and S. R. Sharpe, Phys. Rev. D **90**, 116003 (2014).
[5] M. T. Hansen and S. R. Sharpe, Phys. Rev. D **92**, 114509 (2015).
[6] M. Lüscher, Nucl. Phys. **B354**, 531 (1991).
[7] K. Rummukainen and S. A. Gottlieb, Nucl. Phys. **B450**, 397 (1995).
[8] P. F. Bedaque, Phys. Lett. B **593**, 82 (2004).
[9] C. h. Kim, C. T. Sachrajda, and S. R. Sharpe, Nucl. Phys. **B727**, 218 (2005).
[10] Z. Fu, Phys. Rev. D **85**, 014506 (2012).
[11] L. Leskovec and S. Prelovsek, Phys. Rev. D **85**, 114507 (2012).
[12] M. Göckeler, R. Horsley, M. Lage, U. G. Meißner, P. E. L. Rakow, A. Rusetsky, G. Schierholz, and J. M. Zanotti, Phys. Rev. D **86**, 094513 (2012).
[13] S. He, X. Feng, and C. Liu, J. High Energy Phys. 07 (2005) 011.
[14] M. Lage, U.-G. Meißner, and A. Rusetsky, Phys. Lett. B **681**, 439 (2009).
[15] V. Bernard, M. Lage, U.-G. Meißner, and A. Rusetsky, J. High Energy Phys. 01 (**2011**) 019.
[16] M. Döring, U.-G. Meißner, E. Oset, and A. Rusetsky, Eur. Phys. J. A **47**, 139 (2011).
[17] M. Döring and U.-G. Meißner, J. High Energy Phys. 01 (2012) 009.
[18] D. Agadjanov, U.-G. Meißner, and A. Rusetsky, J. High Energy Phys. 01 (2014) 103.
[19] M. Döring, U.-G. Meißner, E. Oset, and A. Rusetsky, Eur. Phys. J. A **48**, 114 (2012).
[20] M. T. Hansen and S. R. Sharpe, Phys. Rev. D **86**, 016007 (2012).
[21] R. A. Briceño and Z. Davoudi, Phys. Rev. D **88**, 094507 (2013).
[22] P. Guo, J. J. Dudek, R. G. Edwards, and A. P. Szczepaniak, Phys. Rev. D **88**, 014501 (2013).
[23] R. A. Briceño, J. J. Dudek, and R. D. Young, Rev. Mod. Phys. **90**, 025001 (2018).
[24] R. A. Briceño, Phys. Rev. D **89**, 074507 (2014).
[25] F. Romero-López, S. R. Sharpe, T. D. Blanton, R. A. Briceño, and M. T. Hansen, J. High Energy Phys. 10 (2019) 007.
[26] R. A. Briceño, M. T. Hansen, and S. R. Sharpe, Phys. Rev. D **99**, 014516 (2019).
[27] R. A. Briceño, M. T. Hansen, and S. R. Sharpe, Phys. Rev. D **95**, 074510 (2017).
[28] M. T. Hansen and S. R. Sharpe, Annu. Rev. Nucl. Part. Sci. **69**, 65 (2019).
[29] R. A. Briceño, M. T. Hansen, and S. R. Sharpe, Phys. Rev. D **98**, 014506 (2018).
[30] T. D. Blanton, F. Romero-López, and S. R. Sharpe, J. High Energy Phys. 03 (2019) 106.
[31] H.-W. Hammer, J.-Y. Pang, and A. Rusetsky, J. High Energy Phys. 09 (2017) 109.
[32] H. W. Hammer, J. Y. Pang, and A. Rusetsky, J. High Energy Phys. 10 (2017) 115.
[33] R. A. Briceño and Z. Davoudi, Phys. Rev. D **87**, 094507 (2013).
[34] K. Polejaeva and A. Rusetsky, Eur. Phys. J. A **48**, 67 (2012).
[35] M. Mai and M. Döring, Eur. Phys. J. A **53**, 240 (2017).
[36] P. Guo and V. Gasparian, Phys. Lett. B **774**, 441 (2017).
[37] P. Guo and V. Gasparian, Phys. Rev. D **97**, 014504 (2018).
[38] P. Guo and T. Morris, Phys. Rev. D **99**, 014501 (2019).
[39] F. Romero-López, A. Rusetsky, and C. Urbach, Eur. Phys. J. C **78**, 846 (2018).
[40] A. W. Jackura, S. M. Dawid, C. Fernández-Ramírez, V. Mathieu, M. Mikhasenko, A. Pilloni, S. R. Sharpe, and A. P. Szczepaniak, Phys. Rev. D **100**, 034508 (2019).
[41] R. A. Briceño, M. T. Hansen, S. R. Sharpe, and A. P. Szczepaniak, Phys. Rev. D **100**, 054508 (2019).
[42] M. T. Hansen, F. Romero-López, and S. R. Sharpe, J. High Energy Phys. 07 (2020) 047.
[43] T. D. Blanton and S. R. Sharpe, Phys. Rev. D **102**, 054515 (2020).
[44] T. D. Blanton and S. R. Sharpe, Phys. Rev. D **102**, 054520 (2020).
[45] S. Beane *et al.*, arXiv:2003.12130.
[46] S. R. Beane, W. Detmold, T. C. Luu, K. Orginos, M. J. Savage, and A. Torok, Phys. Rev. Lett. **100**, 082004 (2008).
[47] W. Detmold, M. J. Savage, A. Torok, S. R. Beane, T. C. Luu, K. Orginos, and A. Parreno, Phys. Rev. D **78**, 014507 (2008).
[48] W. Detmold, K. Orginos, and Z. Shi, Phys. Rev. D **86**, 054507 (2012).
[49] M. Mai and M. Döring, Phys. Rev. Lett. **122**, 062503 (2019).
[50] T. D. Blanton, F. Romero-López, and S. R. Sharpe, Phys. Rev. Lett. **124**, 032001 (2020).
[51] M. Mai, M. Döring, C. Culver, and A. Alexandru, Phys. Rev. D **101**, 054510 (2020).
[52] P. Guo and B. Long, Phys. Rev. D **101**, 094510 (2020).
[53] B. Hörz and A. Hanlon, Phys. Rev. Lett. **123**, 142002 (2019).
[54] C. Culver, M. Mai, R. Brett, A. Alexandru, and M. Döring, Phys. Rev. D **101**, 114507 (2020).
[55] M. Fischer, B. Kostrzewa, L. Liu, F. Romero-López, M. Ueding, and C. Urbach, arXiv:2008.03035.
[56] See Supplemental Material at http://link.aps.org/supplemental/10.1103/PhysRevLett.126.012001 for additional information concerning the calculation presented in the main letter including details on the extracted finite-volume energies, with a full account of the operator basis used, as well as a thorough description of the fits used to extract the K matrices and of the strategy for, and the results

from, solving the integral equations needed to extract the scattering amplitude.

[57] J. J. Dudek, R. G. Edwards, and C. E. Thomas, Phys. Rev. D **86**, 034031 (2012).

[58] R. G. Edwards, B. Joo, and H.-W. Lin, Phys. Rev. D **78**, 054501 (2008).

[59] H.-W. Lin *et al.* (Hadron Spectrum Collaboration), Phys. Rev. D **79**, 034502 (2009).

[60] R. G. Edwards, J. J. Dudek, D. G. Richards, and S. J. Wallace, Phys. Rev. D **84**, 074508 (2011).

[61] P. Zyla *et al.* (Particle Data Group), Prog. Theor. Exp. Phys. **2020**, 083C01 (2020).

[62] D. J. Wilson, J. J. Dudek, R. G. Edwards, and C. E. Thomas, Phys. Rev. D **91**, 054008 (2015).

[63] R. C. Johnson, Phys. Lett. **114B**, 147 (1982).

[64] D. C. Moore and G. T. Fleming, Phys. Rev. D **73**, 014504 (2006); **74**, 079905(E) (2006).

[65] C. Michael, Nucl. Phys. **B259**, 58 (1985).

[66] M. Lüscher and U. Wolff, Nucl. Phys. **B339**, 222 (1990).

[67] B. Blossier, M. Della Morte, G. von Hippel, T. Mendes, and R. Sommer, J. High Energy Phys. 04 (2009) 094.

[68] J. J. Dudek, R. G. Edwards, N. Mathur, and D. G. Richards, Phys. Rev. D **77**, 034501 (2008).

[69] J. J. Dudek, R. G. Edwards, M. J. Peardon, D. G. Richards, and C. E. Thomas, Phys. Rev. D **82**, 034508 (2010).

[70] J. J. Dudek, R. G. Edwards, and C. E. Thomas (Hadron Spectrum Collaboration), Phys. Rev. D **87**, 034505 (2013); **90**, 099902(E) (2014).

[71] R. A. Briceño, J. J. Dudek, R. G. Edwards, C. J. Shultz, C. E. Thomas, and D. J. Wilson, Phys. Rev. Lett. **115**, 242001 (2015).

[72] R. A. Briceño, J. J. Dudek, R. G. Edwards, C. J. Shultz, C. E. Thomas, and D. J. Wilson, Phys. Rev. D **93**, 114508 (2016).

[73] R. A. Briceño, J. J. Dudek, R. G. Edwards, and D. J. Wilson, Phys. Rev. Lett. **118**, 022002 (2017).

[74] J. J. Dudek, R. G. Edwards, and D. J. Wilson (Hadron Spectrum Collaboration), Phys. Rev. D **93**, 094506 (2016).

[75] G. Moir, M. Peardon, S. M. Ryan, C. E. Thomas, and D. J. Wilson, J. High Energy Phys. 10 (2016) 011.

[76] A. J. Woss and C. E. Thomas, in *Proceedings, 34th International Symposium on Lattice Field Theory (Lattice 2016): Southampton, UK, 2016*; *Proc. Sci.*, LATTICE2016 (2016) 134 [arXiv:1612.05437].

[77] R. A. Briceño, J. J. Dudek, R. G. Edwards, and D. J. Wilson, Phys. Rev. D **97**, 054513 (2018).

[78] A. Woss, C. E. Thomas, J. J. Dudek, R. G. Edwards, and D. J. Wilson, J. High Energy Phys. 07 (2018) 043.

[79] D. J. Wilson, R. A. Briceño, J. J. Dudek, R. G. Edwards, and C. E. Thomas, Phys. Rev. D **92**, 094502 (2015).

[80] G. K. C. Cheung, C. O'Hara, G. Moir, M. Peardon, S. M. Ryan, C. E. Thomas, and D. Tims (Hadron Spectrum Collaboration), J. High Energy Phys. 12 (2016) 089.

[81] D. J. Wilson, R. A. Briceño, J. J. Dudek, R. G. Edwards, and C. E. Thomas, Phys. Rev. Lett. **123**, 042002 (2019).

[82] A. J. Woss, C. E. Thomas, J. J. Dudek, R. G. Edwards, and D. J. Wilson, Phys. Rev. D **100**, 054506 (2019).

[83] M. Peardon, J. Bulava, J. Foley, C. Morningstar, J. Dudek, R. G. Edwards, B. Joo, H.-W. Lin, D. G. Richards, and K. J. Juge (Hadron Spectrum Collaboration), Phys. Rev. D **80**, 054506 (2009).

[84] A. Jackura, C. Fernández-Ramírez, V. Mathieu, M. Mikhasenko, J. Nys, A. Pilloni, K. Saldaña, N. Sherrill, and A. P. Szczepaniak (JPAC Collaboration), Eur. Phys. J. C **79**, 56 (2019).

[85] D. Sadasivan, M. Mai, H. Akdag, and M. Döring, Phys. Rev. D **101**, 094018 (2020).

[86] R. G. Edwards and B. Joo (SciDAC, LHPC, and UKQCD Collaborations), *Lattice field theory. Proceedings, 22nd International Symposium, Lattice 2004, Batavia, USA, 2004*; Nucl. Phys. B, Proc. Suppl. **140**, 832 (2005).

[87] M. A. Clark, R. Babich, K. Barros, R. C. Brower, and C. Rebbi, Comput. Phys. Commun. **181**, 1517 (2010).

[88] R. Babich, M. A. Clark, and B. Joo, in SC 10 (Supercomputing 2010) New Orleans, Louisiana, 2010 (2010) [arXiv:1011.0024].

[89] M. A. Clark, B. Joó, A. Strelchenko, M. Cheng, A. Gambhir, and R. C. Brower, in *SC '16: Proceedings of the International Conference for High Performance Computing, Networking, Storage and Analysis* (2016), pp. 795–806.